An initial assessment of porous metal foam liners for acoustic broadband damping

Fleming Kohlenberg[1], Karsten Knobloch[1]
[1] German Aerospace Center, Dept. of Engine Acoustics, 10623 Berlin, Email: fleming.kohlenberg@dlr.de

Introduction

The noise spectrum of future aircraft engines is expected to be more broadband and less dominated by tonal content due to advances in fan blade technology. Conventional liners excel at damping at their respective Helmholtz resonances with suboptimal broadband damping. This is where porous structures exhibit superior performance. They are commonly used in architectural acoustics and HVAC systems. However, their applicability to aircraft engines has been limited due to the harsh environment (temperature, fluids, bird strike, etc.). A promising bridge is the use of highly porous metal foam liners that are able to withstand these conditions while offering significant broadband damping.

Metal foams are lightweight, recyclable, and resistant to fluids, impacts, and high temperatures. They are used as filters, heat exchangers, electrodes, and, if open-celled, as sound absorbers. Metal foams are manufactured either by foaming with a blowing agent or using space holders that are leached out via dissolution. The most important geometrical features affecting absorption are the porosity and pore size. The porosity $\Phi = 1 - \rho_b/\rho_s$ can be estimated with the bulk density ρ_b, which includes the air in the pores and the skeletal material ρ_s.

Another important parameter is the pore size. Altering the pore size changes the surface area and hence the thermal and viscous behaviour. Han et al. showed that a smaller pore size leads to higher absorption due to increased flow resistance and that a graded pore size might be beneficial to reduce reflection [1]. Lomte et al. investigated the acoustic effect of compressing metal foams, thereby altering their density, pore size, and flow resistivity [2]. They showed that higher damping is achievable by combining multiple different samples. In the context of aircraft noise reduction, Sutliff et al. investigated metal foams as over-the-rotor liners to reduce noise sources in the vicinity of the fan [3]. They investigated metal foams with densities between 6–8 % and pore sizes ranging from 20–100 pores per inch (ppi). They found an optimum value for their application with 8 % density and a pore size of 80 ppi.

This submission deals with the experimental characterisation of metal foam probes and their acoustic properties in the context of a future application in an aero-engine. This includes the determination of the probe's flow resistance, absorption and dissipation of sound by taking advantage of the multiple test-rigs of the German Aerospace Center in Berlin.

Modeling and characterization

There exist multiple models to predict the impedance

$$\zeta = -\mathrm{i}\zeta_\mathrm{c} \cot k_\mathrm{c} t \tag{1}$$

of a porous sample with the thickness t. They differ in their degree of empiricism and which physical absorption effects are taken into account to predict the normalized characteristic impedance ζ_c and wavenumber k_c. A very simple empirical model for fibrous media is from Delany, Bazley and Miki [4]:

$$\zeta_\mathrm{c} = (1 + 0.07\left(\frac{f}{\sigma}\right)^{-0.632} - \mathrm{i}0.107\left(\frac{f}{\sigma}\right)^{0.632}) \tag{2}$$

$$k_\mathrm{c} = -\mathrm{i}k_0\left[0.16\left(\frac{f}{\sigma}\right)^{-0.618} + \mathrm{i}\left(1 + 0.109\left(\frac{f}{\sigma}\right)^{-0.618}\right)\right]. \tag{3}$$

This model only requires knowledge of the flow resistivity σ but is restricted to materials with porosity $\Phi \approx 1$, $\rho_0 f/\sigma \in [0.01, 1]$, and $\sigma \in [1000, 50000]$ in $\mathrm{Pa\,s\,/\,m^2}$. A more complex model is the semi-phenomenological Johnson-Champoux-Allard-Lafarge (JCAL) model which includes visco-inertial and thermal effects for a medium with a motionless skeleton and arbitrary pore shapes. However, it requires six empirical parameters, which cannot be measured directly but can be estimated from normal impedance measurements.

The normalised characteristic impedance ζ_c and wavenumber k_c of homogeneous structures can be determined experimentally, e.g. by using a transmission tube with a transfer matrix approach or the two-thickness method [5]. Using two samples, with one sample having twice the thickness of the first sample $t_2 = 2t_1$, one can use

$$\zeta_\mathrm{c} = \sqrt{\zeta_1(2\zeta_2 - \zeta_1)} \tag{4}$$

$$k_\mathrm{c} = \frac{-\mathrm{i}}{t_2}\ln\left[\frac{1+a}{1-a}\right], \quad \text{with } a = \sqrt{\frac{2\zeta_2 - \zeta_1}{\zeta_1}} \tag{5}$$

to determine the sample impedance, independent from the sample thickness. $\zeta_{1,2}$ denotes the measured surface impedance of the respective sample.

Raylometer

We used a simple flow duct setup (Fig. 1) to determine the flow resistivities of different porous samples. The airflow resistivity $\sigma = \Delta p/vt$ is a measure of the resistance against the permeation of a static fluid flow, which is specific for each porous material and to some degree due to its random structure specific for each sample, but independent of the sample thickness t[6]. The pressure difference Δp is measured by a MKS Baratron 120D with range 1333.2 Pa and the airflow velocity v is controlled by a Bronkhorst Inflow 1 kg/h and Bronkhorst Inflow 20 kg/h mass flow controller. The measurable range of airflow velocity is

6.5−3000 mm/s. In agreement with ISO 9053, the measurement values were extrapolated down to 0.5 mm/s to obtain the linear static airflow resistance σ_0.

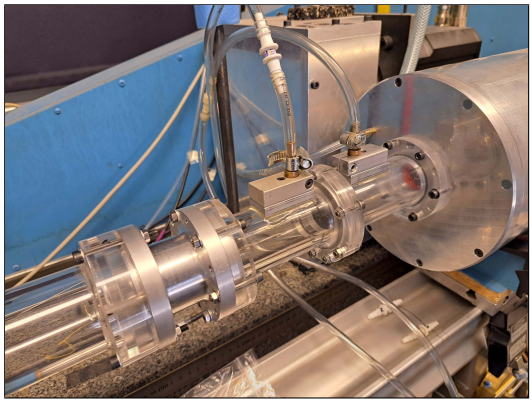

Figure 1: Raylometer

Normal Incidence Tube (D-NIT)

We determined the absorption and surface impedance of the porous metal samples using the normal incidence tube (D-NIT) of the Department of Engine Acoustics of the German Aerospace Center (DLR-AT-TRA) in Berlin, as depicted in Fig. 2. The normal incidence impedance

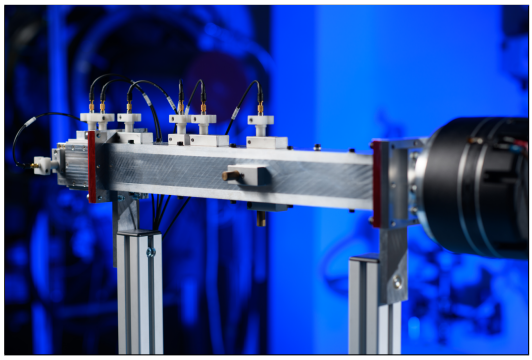

Figure 2: Normal incidence tube D-NIT

tube has a square cross-section of 35 mm × 35 mm and therefore a cut-on frequency of the first higher mode of 4900 Hz. The sound source was an upstream loudspeaker (BMS-4599-ND) attached to the duct end opposite to the probe. We used a multi-microphone method with three microphones (G.R.A.S 46BD-FV 1/4") flush mounted in the measurement section to decompose the sound field into incoming and reflecting acoustic waves to calculate the absorption $\alpha = 1 - |r|^2$ and the complex normalised impedance $\zeta = {}^{Z}/_{\rho_0 c_0} = \frac{1+r}{1-r}$, where r is the complex reflection. A more detailed characterisation of the test rig can be found in [7].

Duct Acoustic Test Rig (DUCT-R)

The acoustic properties of selected metal foam liners in a grazing incidence setup were investigated at the duct acoustic test rig (DUCT-R) facility of the German Aerospace Center (DLR) in Berlin. The rig is depicted in Fig. 3 and consists of two symmetrical parts, each equipped with a loudspeaker and five flush-mounted microphones for plane wave decomposition, with a cross section of 60 mm × 80 mm and a cut-on frequency of the first higher mode of 2142 Hz at ambient conditions. The

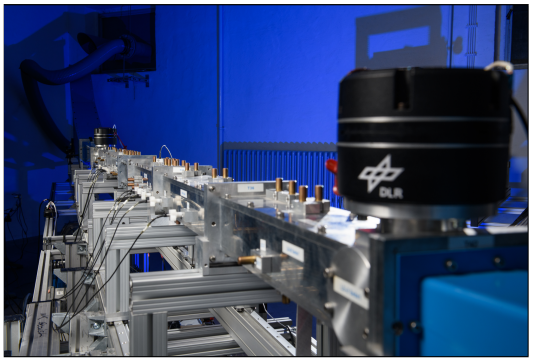

Figure 3: Duct acoustic test rig DUCT-R

decomposed sound field before and after the test section was used to determine the energetic scattering coefficients (reflection R, transmission T, dissipation Δ) upstream and downstream of the channel with the liner installed at one side of the duct. Note that the dissipation is calculated as $\Delta = 1 - R - T$, i.e., acoustic energy neither reflected nor transmitted has to be dissipated by the liner.
The test facility offers the possibility to measure the effect of grazing flow and nonlinear sound excitation with sound amplitudes of more than 130 dB. More information about the test rig can be found in [8].

Samples

The investigated open porous metal samples are listed in Table 1. The diverse materials can be grouped into three categories. The first group (Inc) consists of highly porous samples made of Inconel, which is thrice as heavy as aluminium. The second category (Al-L) consists of three samples of aluminium with a lower porosity of about 60 % and lower pores per inch (ppi). Aluminium foam samples with high porosity constitute the third category (Al-H). The different materials were prepared to fit into

Table 1: Porous metal samples

Group	Name	Porosity in %	Pore size in ppi
Inconel	Inc-1	89	unkn.
$\rho = 8.4\,\mathrm{g/cm^3}$	Inc-2	90	unkn.
Aluminium	Al-L-1	56-60	3-5
Low porosity	Al-L-2	56-60	2-3
$\rho = 2.7\,\mathrm{g/cm^3}$	Al-L-3	56-60	4-8 & 1
Aluminium	Al-H-1	92-94	40
High porosity	Al-H-2	76-88	40
$\rho = 2.7\,\mathrm{g/cm^3}$	Al-H-3	91	unkn.
	Al-H-4	91	unkn.

the Raylometer, D-NIT and DUCT-R. Representative metal samples for each group prepared for D-NIT are depicted in Fig. 4.

Figure 4: Porous metal samples Inc-1 (left), Al-L-1 (middle) and Al-H-1 (right)

Results

Figure 5 depicts the measured flow resistivities in the Raylometer. The three material groups cover a large range of different flow resistivities, with AL-L having the largest ($> 20\,000\,\mathrm{Pa\,s/m^2}$), Inc intermediate ($\approx 10\,000\,\mathrm{Pa\,s/m^2}$) and AL-H having the lowest ($< 500\,\mathrm{Pa\,s/m^2}$) values. The porosity and pore size both affect the flow resistivity, which is visible when comparing AL-H-1 vs. Al-H-2 and Inc-1 vs. Al-H-1, assuming that the sample material is irrelevant since absorption is due to viscothermal losses and not structural vibration. The flow resistivity increased linearly with v, except at very low velocities. The latter is a problem for the linear extrapolation down to 0.5 mm/s to obtain the linear static airflow resistance.[1] The absorption spectra, as measured in D-NIT, of all samples with a thickness of roughly 10 mm is depicted in Fig. 6. The absorption spectra of all samples rose with frequency and showed similar trends as those of the flow resistivity. Therefore, a sufficiently high flow resistivity is critical for substantial sound absorption. Note that the Al-L samples have roughly 1.5 times the weight of the Inc samples. We used our measured flow resistivity to predict the absorption using the Miki model (Eq. (2)). A comparison with the absorption measured in D-NIT for a representative material from each group is depicted in Fig. 7. The absorption spectra of the Inc samples agreed very well. This holds true for the AL-H samples at low frequencies, as well. However, for AL-H at $f > 1750\,\mathrm{Hz}$ the Miki model fails, since $\rho_0 f/\sigma > 1$. The Miki model failed to predict the absorption of the AL-L samples because its porosity is much lower than 1. Therefore, for materials such as AL-L, higher fidelity models are needed.

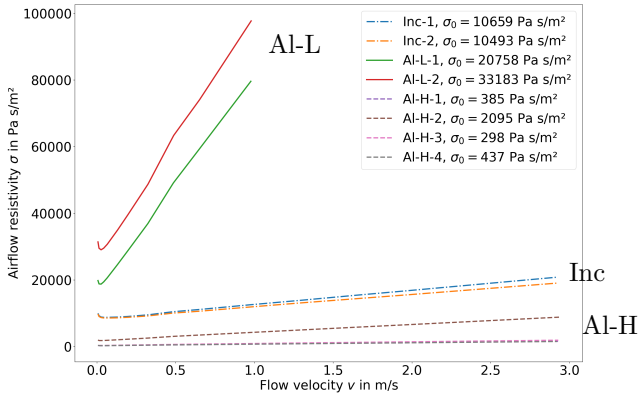

Figure 5: Flow resistivity

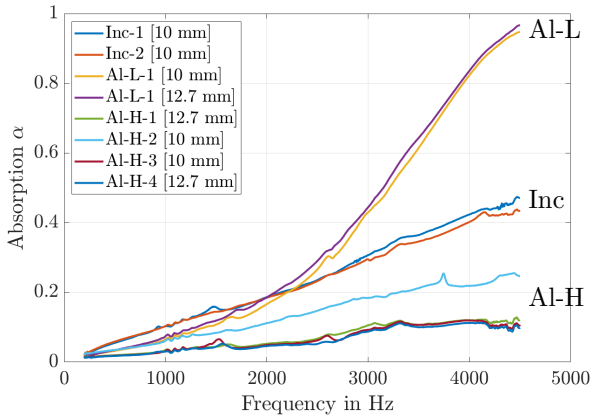

Figure 6: Normal incidence absorption

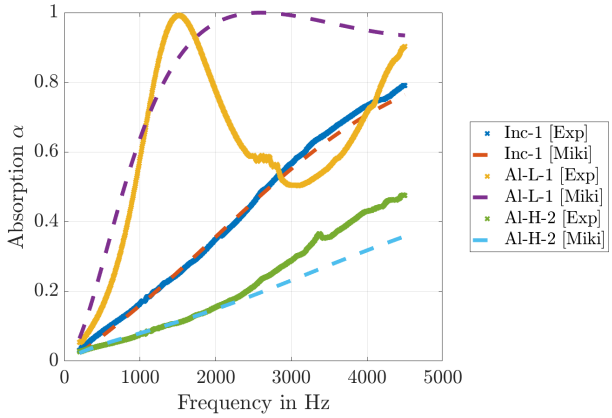

Figure 7: Measured versus simulated absorption using Miki model

We stacked up to three samples to evaluate different thicknesses for each material. We used two for the two-thickness method to extract the thickness-independent acoustic properties (Eq. (4)) and used this information with (Eq. (1)) to model the impedance of the third thickness. A comparison is depicted in Fig. 8. The two thickness method works well for the Inc and Al-L samples. However,

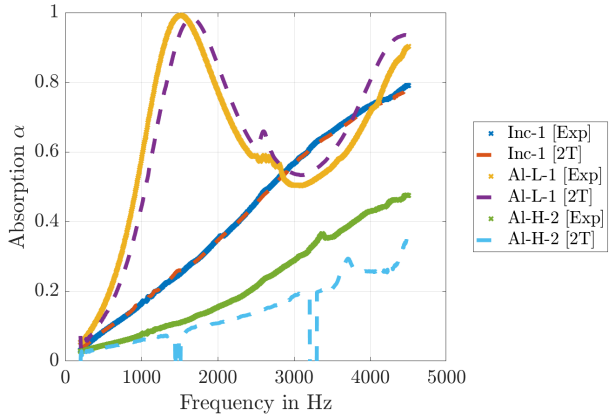

Figure 8: Measured versus simulated absorption using Two-Thickness method

[1] Note, that a plane wave with an amplitude of 80 dB has a sound particle velocity of 0.5 mm/s while 1 m/s corresponds to 146 dB.

for AL-H the absorption is too low to distinguish between the different thicknesses. The dropouts around 1600 Hz and 3200 Hz hint at resonances where the method fails. It is interesting to note, that both the two thickness method, as well as the Miki model under-predict the absorption of the AL-H samples.

The scattering coefficients of the Inc sample with two different thicknesses (15 mm and 30 mm) obtained at DUCT-R without flow are depicted in Fig. 9. The reduction

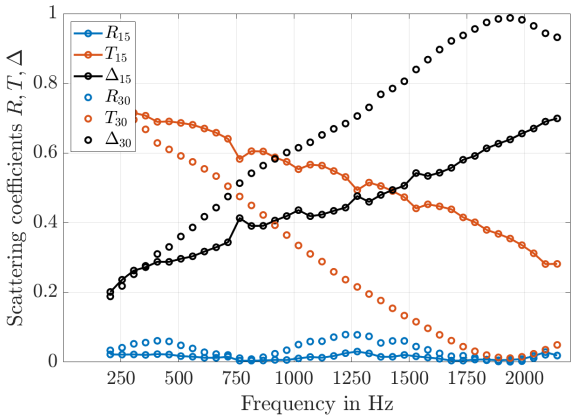

Figure 9: Scattering coefficients (No Flow)

of transmitted energy (red) is due to dissipative effects (black) because the reflection (blue) is very low. Similar to absorption, dissipation increased with frequency. The thicker sample allows for greater dissipation. The effect is stronger at higher frequencies. The other materials show similar trends but are omitted here for the sake of brevity. The effect of a grazing flow with a centreline Mach number of 0.3 is depicted in Fig. 10. The convection effects of

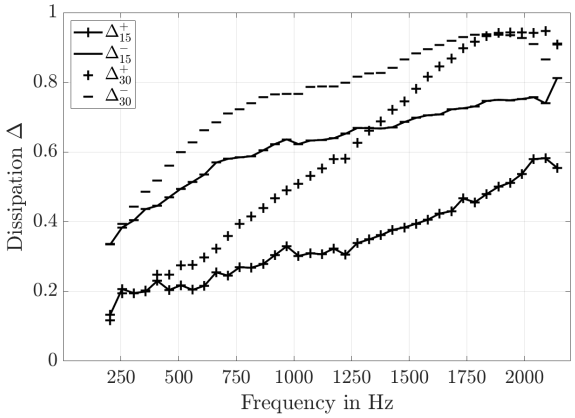

Figure 10: Scattering coefficients (Ma = 0.3)

the grazing flow led to higher damping against the flow direction (minus) than in the flow direction (plus). The general spectrum shape is shifted but remains similar to that of the no-flow case. Again, the effect is stronger at higher frequencies.

Conclusion

We characterised a wide range of porous metals in terms of their acoustic damping ability and flow resistivity. We found that high-porosity inconel samples exhibited good damping at high frequencies. In contrast, highly porous aluminium foams with different pore sizes exhibited poor damping due to their low flow resistivity. Finally, aluminium samples with lower porosity showed good mid-frequency damping but could not be modelled with the Miki model. In future work, we will focus on damping improvements by using a backing air cavity and tailored materials with a density gradient for better impedance matching.

Acknowledgements

This work was mainly funded within the DLR project LU(FT)² 2030 [Leises Umwelt-Freundliches Transportflugzeug durch Fortschrittliche Technologiesimulation für 2030]. The authors want to thank Sebastian Kruck from the DLR workshop team for his support in the sample and measurement setup preparation.

References

[1] Han, Fusheng; Seiffert, Gary; Zhao, Yuyuan; Gibbs, Barry (2003): Acoustic absorption behaviour of an open-celled aluminium foam. In: J. Phys. D: Appl. Phys. 36 (3), S. 294–302. DOI: 10.1088/0022-3727/36/3/312.

[2] Lomte, Amulya; Sharma, Bhisham; Drouin, Mary; Schaffarzick, Denver (2022): Sound absorption and transmission loss properties of open-celled aluminum foams with stepwise relative density gradients. In: Applied Acoustics 193. DOI: 10.1016/j.apacoust.2022.108780.

[3] Sutliff, Daniel L.; Jones, Michael G.; Hartley, Thomas C. (2013): High-Speed Turbofan Noise Reduction Using Foam-Metal Liner Over-the-Rotor. In: Journal of Aircraft 50 (5), S. 1491–1503. DOI: 10.2514/1.C032021.

[4] Miki, Yasushi (1990): Acoustical properties of porous materials. Modifications of Delany-Bazley models. In: J. Acoust. Soc. Jpn. (E), J Acoust Soc Jpn E 11 (1), S. 19–24. DOI: 10.1250/ast.11.19.

[5] Smith, Charles D.; Parrott, Tony L. (1983): Comparison of three methods for measuring acoustic properties of bulk materials. In: The Journal of the Acoustical Society of America 74 (5), S. 1577–1582. DOI: 10.1121/1.390119.

[6] Acoustics - Determination of airflow resistance - Part 1: Static airflow method (ISO 9053-1:2018)

[7] Kohlenberg, Fleming; Knobloch, Karsten (2024): Experimental and Numerical Parameter Study of a Helmholtz Resonator with a Flexible Wall. In: 30th AIAA/CEAS Aeroacoustics Conference (2024). Rome, Italy

[8] Busse-Gerstengabe et. al.: Comparative study of impedance eduction methods, Part 1: DLR tests and methodology. (19th AIAA/CEAS Aeroacoustics Conference 2013) AIAA-2013-2124